Photodiagnosis and Photodynamic Therapy 26 (2019) 361–365

Contents lists available at ScienceDirect

Photodiagnosis and Photodynamic Therapy

journal homepage: www.elsevier.com/locate/pdpdt

Subphthalocyanine as a fluorescence imaging agent for breast tumor

Fatma Yurt[a,*], Mine Ince[b], Ozge Er[a], Hale Melis Soylu[c], Kasim Ocakoglu[b,*], Osman Yilmaz[d]

[a] Department of Nuclear Applications, Institute of Nuclear Science, Ege University, Bornova, 35100, Izmir, Turkey
[b] Department of Energy Systems Engineering, Faculty of Technology, Tarsus University, 33400, Tarsus, Turkey
[c] Department of Biomedical Technology, Institute of Science, Ege University, Bornova, 35100, Izmir, Turkey
[d] Department of Animal Research Center, Dokuz Eylul University, 35340, Izmir, Turkey

ARTICLE INFO

Keywords:
Subphthalocyanine
Fluorescence imaging
Mammary tumor
Nude mice

ABSTRACT

Tri-*tert*-butyl-carboxyl subphthalocyanine (SubPc) was synthesized and evaluated as a fluorescence agent. Fluorescence imaging for breast tumor *in vivo* was performed using nude mice as models. Results indicate high uptake in tumor at 20 h. Tumor-non tumor ratio was determined as 2.25. The imaging results demonstrate the potential of this fluorescence-imaging agent in the diagnosis of breast tumor. In the future, subphthalocyanine is also developing as a dual functional, which is fluorescence imaging and as a photodynamic therapeutic agent for the treatment and diagnosis of cancer.

1. Introduction

Mammary cancer can exhibit a high mortality rate among patients. Early diagnosis of the disease is vitally important to increase the success of therapy. Imaging has been an essential approach to assist in the staging of cancer. Ultrasonography, computed tomography (CT), magnetic resonance and nuclear imaging are useful diagnostic methods for cancer imaging. Fluorescence imaging is a novel imaging method with many possible advantages such as low cost, high sensitivity and non-invasiveness. Thereby, it could be used widely as a medical imaging technique. Molecular probes can apply deep penetration into organs for imaging fluorescence since organs have low scattering effect and background interference. Moreover, fluorescent probe molecules have been used in photodynamic therapy (PDT) as a noninvasive tool for cancer therapy [1–3]. Zinc phthalocyanines have been used as optical probes due to its intense fluorescence emission in the red part of the visible region. They have received significant research interest and widely investigated in, biomedical sciences and material sciences because of their properties. Zinc phthalocyanines were also applied as PDT agents to treat cancer and infection [4–9]. On the other hand, SubPcs exhibit more intense fluorescence signals compared to Ps or phthalocyanines (Pcs), which may be exploited in efficientfluorescent labeling of living cells [10,11]. Additionally, SubPcs have outstanding photophysical features, such as intense fluorescence emission and photosensitizing properties [12]. On the other hand, subphthalocyanines are preferred in such application due to their bowl-shaped structures restrict pi-pi stacking that can quench the fluorescence [13]. In our current study, we have synthesized subphthalocyanine and *in vivo* fluorescence imaging potential was evaluated in breast tumor bearing nude mice.

2. Material and methods

The synthesis of symmetrically substituted SubPc derivatives is based on the cyclotrimerization of corresponding phthalonitrile precursor in the presence of boron reagents in high boiling point of solvent such as *p*-xylene. Tri-*tert*-butyl-carboxysubphthalocyanine (SubPc) was prepared according to the previously published method using 4-*tert*-butyl phthalonitrile and BCl_3 in p-xylene [14]. The reaction was followed by nucleophilic substitution of the axial chlorine atom with corresponding aldehyde in toluene. The oxidation of aldehyde derivative led to desired SubPc, which axially functionalized with carboxy groups. The chemical structure of tri-*tart*-butyl-carboxy SubPc as shown in Fig. 1. All chemicals were purchased from Sigma-Aldrich.

2.1. UV–vis and fluorescence spectra of subphthalocyanine

UV–vis spectra were recorded with an Analytic JENA S 600 UV–vis spectrophotometer. The solution of SubPc in $CHCl_3$ was used for UV measurements. The absorption wavelength of SubPc was recorded as 568 nm (Fig. 2a). Fluorescence spectra was recorded on a Shimadzu RF-5301 PC spectra fluorophotometer (Kyoto, Japan). One mg of SubPc was dissolved in 10 mL DMSO and 5 mL of SubPc solution was taken for fluorescence measurements. The spectra show that excitation and

* Corresponding authors.
E-mail addresses: fatma.yurt.lambrecht@ege.edu.tr (F. Yurt), kasim.ocakoglu@tarsus.edu.tr (K. Ocakoglu).

https://doi.org/10.1016/j.pdpdt.2019.04.022
Received 10 October 2018; Received in revised form 22 April 2019; Accepted 22 April 2019
Available online 24 April 2019

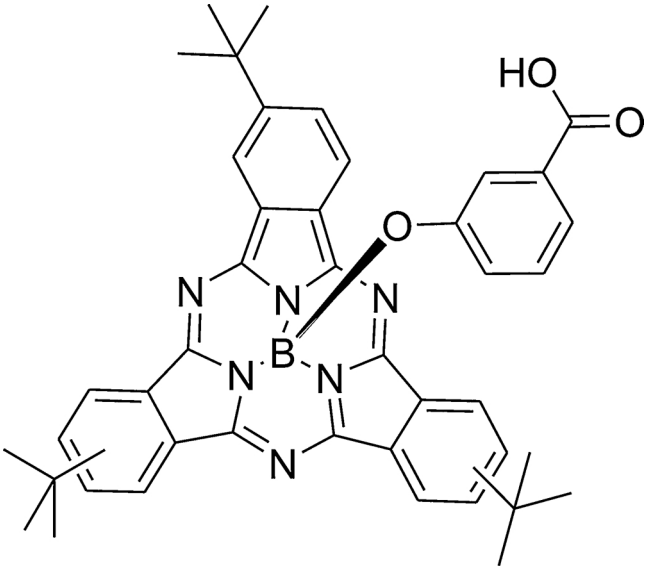

Fig. 1. The chemical structure of tri-*tert*-butyl-carboxy SubPc.

emission wavelengths are 505 and 601 nm respectively (Fig. 2b).

2.2. Animals and tumors

This animal study was approved by animal research local ethics committee of Ege University. Ethical rules and procedures were applied to all animals. Athymic nude mice (Foxn1nu/Foxn1 + , 5–6 weeks, female, 25–30 g) were purchased from Kobay A.Ş. They were kept in sterilized special cages with hepafilter. Animals had free access sterile water and food.

Cells of mouse mammary carcinoma (EMT6, ATCC, CRL2755) were incubated in 75 cm^2 flasks in 5% CO_2 incubator at 37 °C with Minimum Essential Medium (MEM). Cells were removed by cell scaber from the flasks when they were in 90% confluence, without trypsin. 1×10^7 cells in 0.5 cc incomplete medium per animal were injected subcutaneous to lateral lower back of the animals by insulin injector. Mice were observed about tumor growth, body weight and clinical observation. Tumors reached to 15 mm diameter within 8–10 days.

2.3. In vivo imaging and biodistribution of SubPc

Subphthalocyanine (0.63 μmol/10 μL, DMSO) was diluted to 100 μL with deionized water and the solution was intravenously injected into the tail vein of nude mice. Nude mice with tumor were randomly assigned to different grouses follows: intravenous injection and control group (n = 3 for each group). The mice were anesthetized with 2.5% isoflurane with 1% oxygen during the imaging session. Images were taken using IVIS spectrum (PerkinElmer) (excitation 500 nm and emission 620 nm) with an exposure time of 3 s in 30 min, 120 min, 360 min, and 20 h. At the end of the imaging, anesthetized nude mice were sacrificed and images of organs were carried out evaluate the distribution of SubPc. The organs and tumor were excised and imaged ex vivo using 2D fluorescent imaging employing a filter pair of 500/620 nm for fluorescence efficiency quantification. Other leg muscle (without tumor) was used as control tissue. All images were analyzed using *in vivo* imaging software.

3. Results and discussion

3.1. In vivo imaging of the distribution of SubPc in tumor bearing nude mice

To examine the tumor targeting capability of SubPc *in vivo*, SubPc was intravenously injected into the tumor bearing mice *via* the tail vein. The fluorescence signal and intensity distribution of SubPc were monitored with an *in vivo* fluorescence imaging system. The imaging was given in Fig. 3. As seen in Fig. 3. SubPc biodistribution is very slow throughout the body of the mice in 2 h. The fluorescence intensity increased in tumor, while the signal in other organs reduced rapidly in 20 h. The fluorescence signal is seen in kidneys in 20 h. However, the tumor–to-control ratio is 2.25 and reached the maximum accumulation in 20 h. In the study by Lobo et.al. fluorescence imaging with Pc6 compound was carried out in BALAB/c mouse with 4T1-luc2 tumor [3]. They compared with Pc6 located in the right (with tumor) and left (without tumor) mammary fat pads. As known, this is an important parameter to assess the sensitivity of fluorescence imaging with Pcs. In this study the ratio was found 1.8 at 4 h post iv. Our result is similar also.

In another study of PcZn2-lys-FA in the tumor of KB human tumor bearing BALB/c nude mice was accumulated at 3 h post-injection. The fluorescence intensity had increased in the tumor after 3 h, while the accumulation in some organs (liver, spleen, lung and kidney) reduced rapidly. It is observed that the tumor-to background ratio increased significantly after 7 h [15].

Feng et al. synthesized galactose substituted zinc phthalocyanines and investigated their fluorescence imaging effect in nude mice bearing liver cancer model. In accordance with their imaging results, the maximum fluorescence intensities were obtained from 12 h to 24 h. The excellent tumor imaging of galactose substituted zinc phthalocyanine was found at 24 h after intravenous injection. We found that SubPc uptake reached maximum in tumor at 24 h also. They observed that fluorescence could be detected in the liver, spleen, lung, kidney and tumor from ex vivo study results. Our ex vivo results demonstrated that SubPc accumulated in the tumor and cleared in the organs after 24 h. These organs show weak fluorescence ex vivo, the fluorescence signal in

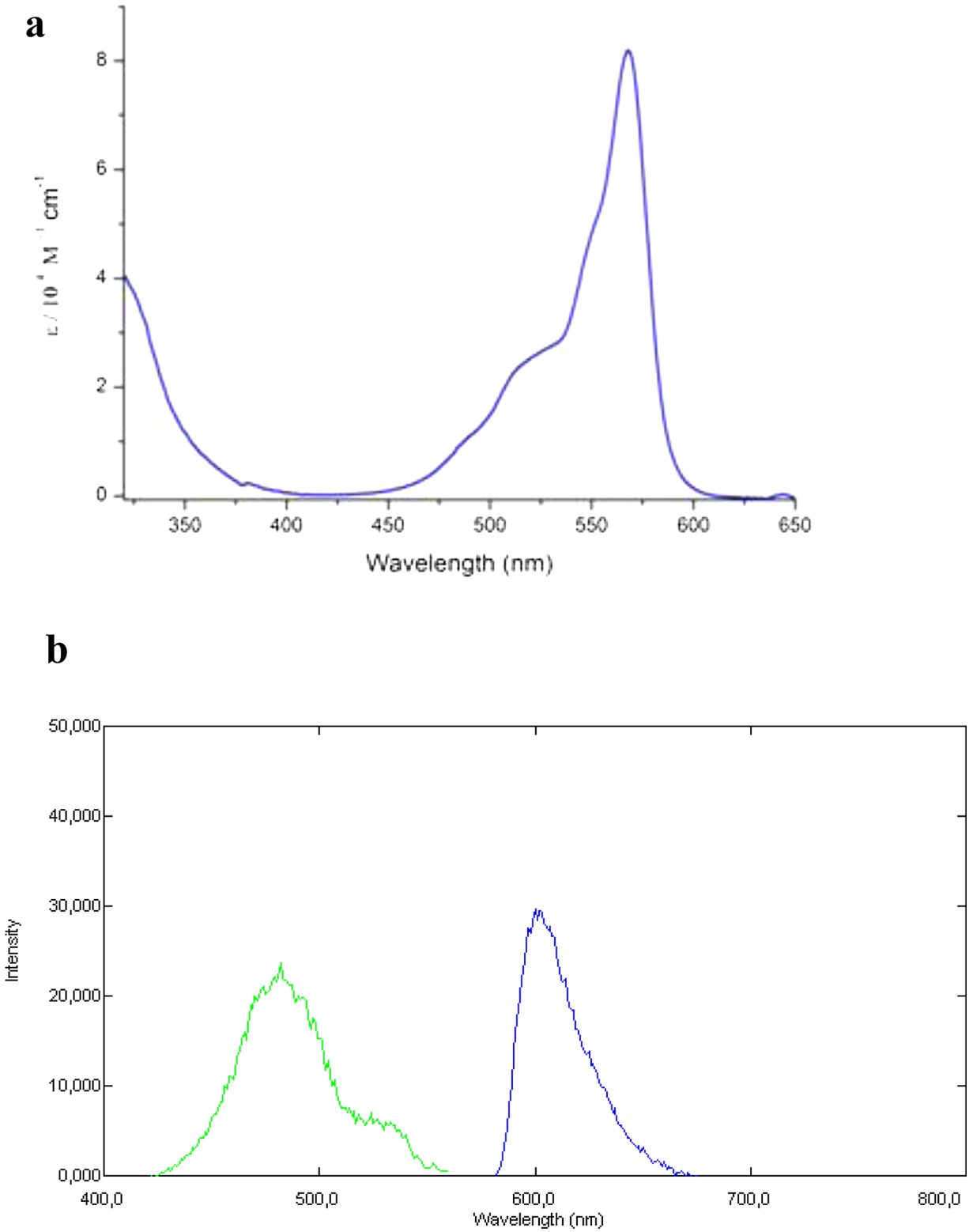

Fig. 2. (a) UV/vis absorption spectra of SubPc in $CHCl_3$ absorption wavelength 568 nm. In **(b)** Fluorescence spectra of subphthalocyanines measured in DMSO. Excitation wavelength 505 nm and emission wavelength 601 nm.

tumor is strong. They found fluorescence intensity in tumor/control ratio was 1.5 by Feng et.al. [16]. The ratio (2.25) that we obtained in our study is higher than theirs. This allows thatthe fluorescence imaging of tumor is easily to be detected.In concluding these initial data provided strong evidence of high specificity tumor targeting.

4. Conclusion

In summary, Subphthalocyanine was synthesized. Fluorescence imaging studies *in vivo* distribution in organs proves that SubPc could be used as fluorescent imaging agent. SubPc can absolutely discriminate

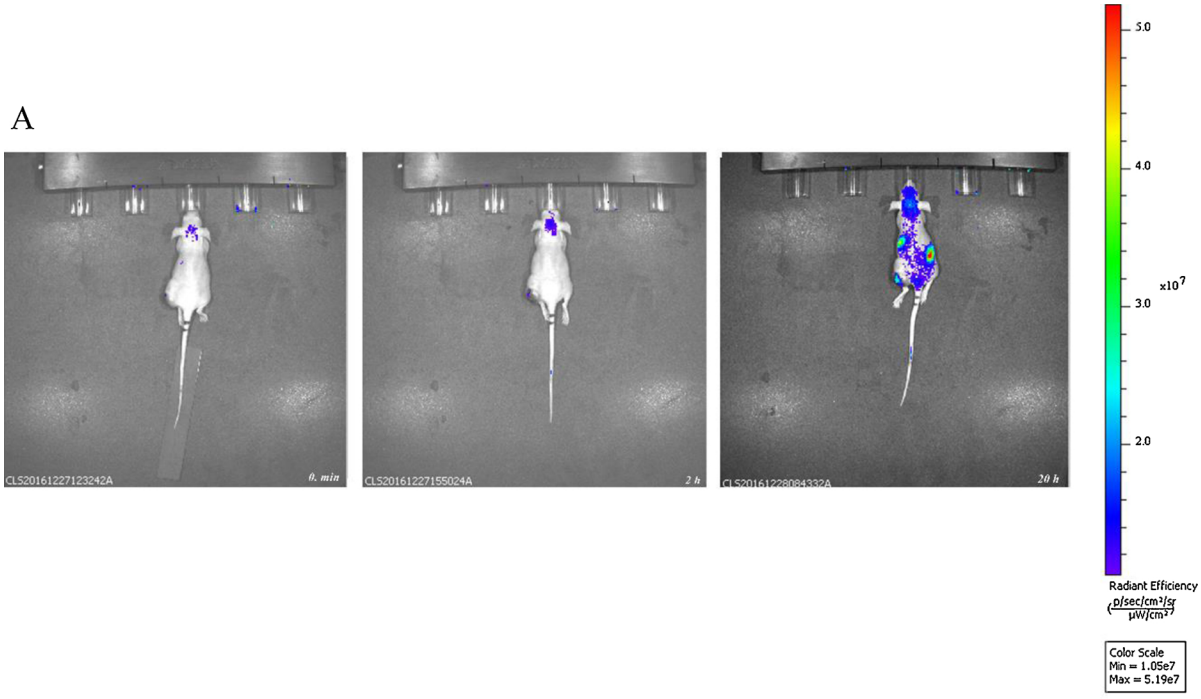

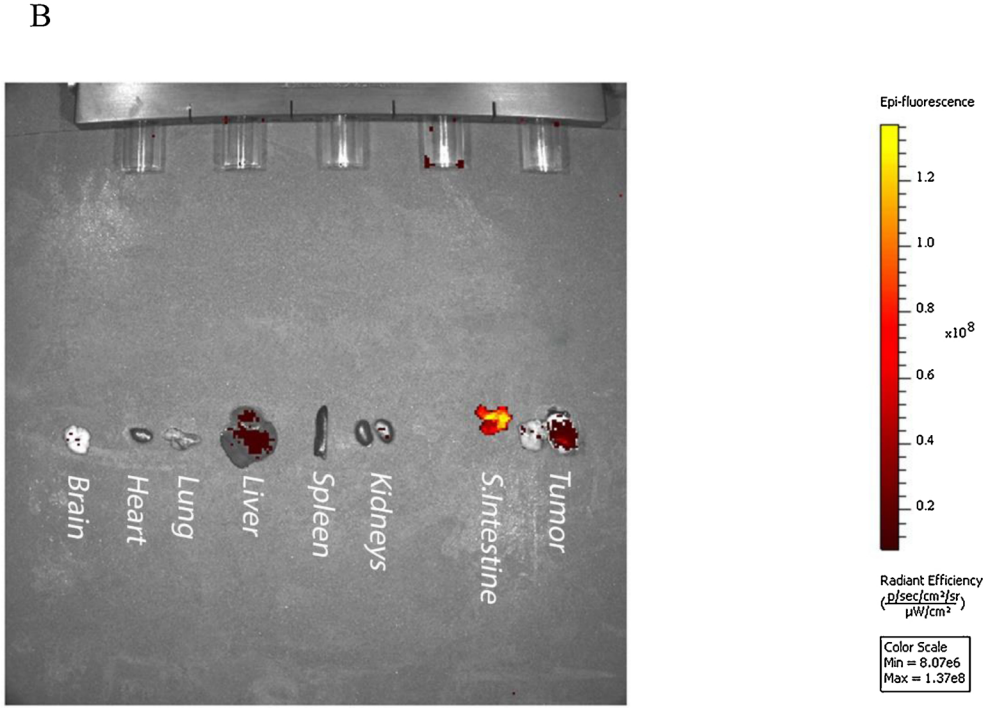

Fig. 3. (**A**) Distribution and fluorescence intensity of dissected organs in 0 h, 2 h and 20 h (**B**) *Ex vivo* imaging in 20 h.

between healthy and tumor tissue in tumor model, making this result a promising therapeutic and fluorescence imaging agent for the treatment and diagnosis of cancer. The current study investigations are preliminary studies in the search for effect photodynamic therapy for breast tumor. These results are promising for the possible development of such SubPc for fluorescence imaging.

References

[1] H. Abramczyk, B. Brozek-Pluska, J. Surmacki, J. Musial, R. Kordek, Oncologic photodynamic diagnosis and therapy: confocal Raman/fluorescence imaging of metal phthalocyanines in human breast cancer tissue in vitro, Analyst 139 (21) (2014) 5547–5559.

[2] L. Lu, F. Lv, B. Cao, X. He, T. Liu, Saccharide substituted zinc phthalocyanines: optical properties, Interaction with bovine serum albumin and near infrared fluorescence imaging for sentinel lymph nodes, Molecules 19 (1) (2014) 525–537.
[3] A.C. Lobo, A.D. Silva Tomé, V.A. Pinto, S.M. Silva, E.F.M.J. Calvete, L.G. Arnaut, Phthalocyanine labels for near-infrared fluorescence imaging of solid tumors, J. Med. Chem. 59 (10) (2016) 4688–4696.
[4] Y. Zhang, J.F. Lovell, Recent applications of phthalocyanines and naphthalocyanines for imaging and therapy. wiley interdisciplinary reviews, Nanomed. Nanobiotechnol. 9 (1) (2017).
[5] A.D. Scully, R.B. Ostler, A.J. MacRobert, A.W. Parker, C.D. Lara, P. O'Neill, D. Phillips, Laser line-scanning confocal fluorescence imaging of the photodynamic action of aluminum and zinc phthalocyanines in V79–4 Chinese Hamster Fibroblasts, Photochem. Photobiol. 68 (2) (1998) 199–204.
[6] G. Avşar, F.A. Sari, A.C. Yuzer, H.M. Soylu, O. Er, M. Ince, F.Y. Lambrecht, Intracellular uptake and fluorescence imaging potential in tumor cell of zinc phthalocyanine, Inter. J. Pharm. 505 (1) (2016) 369–375.
[7] F. Yurt Lambrecht, M. Ince, O. Er, K. Ocakoglu, F. Aslıhan Sarı, C. Kayabasi, C. Gunduz, Dual nuclear/fluorescence imaging potential of zinc (II) phthalocyanine in MIA PaCa-2 cell line, Curr. Radiopharm. 9 (3) (2016) 222–227.
[8] H.L. Van Leengoed, L.M. Van Der Veen, N. Versteeg, A.A.C. Van Der Berg-Blok, A.E. Marijnissen, J.P.A, W.M. Star, Tumour tissue imaging using the localizing properties and fluorescence of some phthalocyanines, Int. J. Radiat. Biol. 60 (1–2) (1991) 121–124.
[9] A.D. Scully, R.B. Ostler, A.J. Mac Robert, A.W. Parker, C.D. Lara, P. O'Neill, D. Phillips, Laser line-scanning confocal fluorescence imaging of the photodynamic action of aluminum and zinc phthalocyanines in V79–4Chinese hamster fibroblasts, Photochem. Photobiol. 68 (2) (1998) 199–204.
[10] Y. Bernhard, P. Winckler, R. Chassagnon, P. Richard, É. Gigot, J.M. Perrier-Cornet, R.A. Decréau, Subphthalocyanines: addressing water-solubility, nano-encapsulation, and activation for optical imaging of B16 melanoma cells, Chem. Commun. (Camb.) 50 (90) (2014) 13975–13978.
[11] I. Roy, D. Shetty, R. Hota, K. Baek, J. Kim, C. Kim, K. Kim, A multifunctional subphthalocyanine nanosphere for targeting, labeling, and killing of antibiotic-resistant bacteria, Angew. Chemie 127 (50) (2015) 15367–15370.
[12] Y. Bernhard, P. Winckler, J.M. Perrier-Cornet, R.A. Decréau, Harnessing medically relevant metals onto water-soluble subphthalocyanines: towards bimodal imaging and theranostics, J. Chem. Soc. Dalton Trans. 44 (7) (2015) 3200–3208.
[13] G.M. Eder, B.R. Walker, P.L. McGrier, Subphthalocyanine-based porous organic polymers, RCS Adv. 7 (47) (2017) 29271–29274.
[14] F. Yurt, F.A. Sarı, M. Ince, S.G. Colak, O. Er, H.M. Soylu, C. Caliskan Kurt, C. Biray Avci, C. Gunduz, K. Ocakoglu, Photodynamic therapy and nuclear imaging activities of SubPhthalocyanine integrated TiO_2 nanoparticles, J. Photochem. Photobiol. A: Chem. 91 (3) (2018) 789–796.
[15] Y. Li, J. Wang, X. Zhang, W. Guo, F. Li, M. Yu, Z. Hong, Highly water-soluble and tumor-targeted photosensitizers for photodynamic therapy, Org. Biomol. Chem. 13 (28) (2015) 7681–7694.
[16] F. Lv, Y. Li, B. Cao, T. Liu, Galactose substituted zinc phthalocyanines as near infrared fluorescence probes for liver cancer imaging, J. Mater. Sci. Mater. Med. 24 (3) (2013) 811–819.